

NASA Technical Memorandum 4588

# Modeling of Instrument Landing System (ILS) Localizer Signal on Runway 25L at Los Angeles International Airport

---

*Richard M. Hueschen and Charles E. Knox  
Langley Research Center • Hampton, Virginia*

National Aeronautics and Space Administration  
Langley Research Center • Hampton, Virginia 23681-0001

---

November 1994

This publication is available from the following sources:

NASA Center for AeroSpace Information  
800 Elkridge Landing Road  
Linthicum Heights, MD 21090-2934  
(301) 621-0390

National Technical Information Service (NTIS)  
5285 Port Royal Road  
Springfield, VA 22161-2171  
(703) 487-4650

## Contents

Summary . . . . .	1
Introduction . . . . .	1
Nomenclature . . . . .	2
Abbreviations . . . . .	2
Symbols . . . . .	2
Description of Test Equipment . . . . .	3
Test Airplane . . . . .	3
FAA RIR-778X Radar Tracker . . . . .	3
ILS System . . . . .	3
Test Design . . . . .	4
Technical Approach . . . . .	4
Flight Paths . . . . .	4
Runway Coordinate System ( $x_{rw}, y_{rw}, z_{rw}$ ) . . . . .	5
Recorded Data . . . . .	5
Data Analysis . . . . .	5
Merging Tracker and Aircraft Data . . . . .	6
Corrections for ILS and transponder antenna locations . . . . .	6
Computation of equivalent localizer deviation . . . . .	7
Conversion of recorded localizer deviation from units of dots to degrees . . . . .	7
Computation of differences between localizer deviations . . . . .	8
Merged Data Analysis . . . . .	8
Analysis of data on perpendicular flight segments . . . . .	8
Analysis of data along runway centerline . . . . .	8
Results . . . . .	8
Perpendicular Flight Segments . . . . .	8
Runway Centerline Flight . . . . .	9
Localizer Contour . . . . .	9
Summary of Results . . . . .	9
Appendix A—Path Waypoints . . . . .	11
Appendix B—Computation of Direction of Line Relative to True North $\psi_N$ . . . . .	12
References . . . . .	14
Figures . . . . .	15



## Summary

A joint NASA/FAA flight test has been made to obtain and develop information suitable for mathematically modeling the localizer signal from an instrument landing system (ILS) at ranges from 10 to 32 n.mi. from the localizer antenna. An additional purpose of the test was to determine and document the location of the ILS localizer signal for future airplane tracking tests. This test was conducted on runway 25L at the Los Angeles International Airport.

During the flight tests, localizer deviations were recorded as the airplane was flown along two pre-programmed paths that had multiple straight-leg segments perpendicular to the runway centerline. The "truth" position of the airplane, as tracked with a precision ground-based radar, was recorded as the airplane was flown along the paths. Differential Global Positioning System (DGPS) navigation was used to ensure that the flight paths were repeatably flown to obtain a consistent set of data for statistical analysis.

The desired lateral portion of the ILS localizer signal recorded corresponded to a difference in depth of modulation equivalent to a signal level of  $\pm 150 \mu\text{A}$  at the ILS receiver output.

The flight test procedures and postflight data analysis performed on the computed differences between the recorded ILS data and recorded precision radar tracking data are described. The data analysis showed that the ILS signal could be suitably modeled with a linear equation. The ILS centerline was found to be offset to the left of runway centerline by  $0.071^\circ$ . No major beam bends were observed in the data although two insignificant beam bends of approximately  $0.01^\circ$  were observed at 12 and 20 n.mi. from the localizer antenna.

## Introduction

Increasing the capability of airports to accommodate more takeoffs and landings is necessary to meet the predicted increase in future air traffic. Studies of Air Traffic Control (ATC) capacity and past experience have indicated that additional parallel runways within current airport boundaries can increase airport capacity without affecting flight safety. Furthermore, additional airport capacity can be achieved as the independence of operations between parallel runways is increased during both visual meteorological conditions (VMC) and instrument meteorological conditions (IMC).

During both VMC and IMC, airplanes may use guidance provided by an instrument landing system

(ILS) to navigate to the runway for a landing. During normal operations, an airplane captures and establishes precision lateral tracking of the ILS localizer signal within 7 to 12 n.mi. of the runway.

If two, or more, parallel ILS approaches to closely spaced parallel runways are being conducted, ATC procedures may require capturing the localizer and beginning the precision tracking at distances greater than 17 n.mi. from the runway. Lateral tracking of the ILS localizer is accomplished with a localizer deviation indicator in the aircraft driven by ILS receiver measurements. These measurements are based on an angular deviation from a reference line (intended to be aligned with the runway centerline) with an apex located at the localizer antenna. As such, sufficient lateral separation between airplanes may not be provided on closely spaced parallel ILS approaches due to the not-well-known ILS angular accuracies at these extended ranges. Sufficient equipment requirements and operational procedures must be developed in simulation and flight testing to accommodate closely spaced parallel ILS approaches.

The Federal Aviation Administration (FAA) and the National Aeronautics and Space Administration (NASA) are currently studying potential airport capacity gains from multiple parallel (more than two) runways. These studies are considering the use of the ILS localizer signal at distances of 30 miles or more from the ILS localizer antenna to effectively conduct closely spaced, multiple parallel ILS approaches. At these extended distances, very little data are available on localizer signal characteristics or airplane localizer tracking accuracy to support these studies. Consequently, the FAA and the NASA conducted a joint flight test to collect data on a typical Category II ILS signal at the extended distances.

This report describes the joint NASA/FAA flight test. The primary objective of the test was to develop information suitable for mathematically modeling a typical Category II ILS localizer for the extended distances from the localizer antenna. A second objective was to determine and document the location of the ILS localizer signal for future airplane tracking tests. To meet these objectives the flight test was conducted on parallel runway 25L at the Los Angeles International Airport (LAX); data were recorded from measurements on the typical Category II ILS installation on that runway.

The desired portion of the ILS localizer signal used for modeling development extended longitudinally between 10 and 32 n.mi. from the localizer antenna. The lateral portion was defined as the area formed between two lines defined by the difference

in depth of modulation (ddm)<sup>1</sup> of  $\pm 150 \mu A$  at the ILS receiver output. These lines equated to two lines approximately  $\pm 1.67^\circ$  on each side of the localizer centerline with the apex at the localizer antenna.

This report describes the test equipment, test design and procedures, and recorded data. Methods for analysis of the recorded data are given followed by results of the analysis.

## Nomenclature

### Abbreviations

ATC	Air Traffic Control
CDU	control display unit (see fig. 4)
CRT	cathode-ray tube
c.g.	center of gravity
DGPS	Differential Global Positioning System
ddm	difference in depth of modulation of ILS 90- and 150-Hz beams
FAA	Federal Aviation Administration
GPS	Global Positioning System
ILS	instrument landing system
IMC	instrument meteorological conditions
LAX	Los Angeles International Airport (Los Angeles, California)
lg	longitude
lt	latitude
MCP	mode control panel (see fig. 4)
MSL	mean sea level
NASA	National Aeronautics and Space Administration
ND	navigation display
PFD	primary flight display
RF	radio frequency
RFD	research flight deck (see fig. 4)
rms	root mean square

<sup>1</sup>Difference in depth of modulation (ddm) is the difference in amplitude of two signals: one modulated at 150 Hz and located predominantly on the right side of the runway centerline and the other at 90 Hz and located predominantly on the left side of the runway centerline. The ddm is proportional to the angle from the runway centerline.

TSRV	Transport Systems Research Vehicle airplane
UTC	universal time coordinated
VMC	visual meteorological conditions

### Symbols

$b, m$	constants (eq. (9))
$d_{cfc}$	difference of localizer measurement and equivalent measurement computed from curve fit of runway centerline path segment data, deg
$d_{cfp}$	difference of localizer measurement and equivalent measurement computed from curve fit of perpendicular path segment data, deg
$d_{loc}$	difference of localizer measurement and equivalent measurement computed from tracker data, deg
$f$	constant to convert from localizer deviation in units of dots to degrees, deg/dot
$h_{MSL}$	height at mean sea level
$\mathbf{r}_A$	vector of dimension $3 \times 1$ of ILS antenna position in runway axes ( $X_{rw}, Y_{rw}, Z_{rw}$ ), ft
$\mathbf{r}_B$	vector of dimension $3 \times 1$ of position of tracker beacon on aircraft, ft
$\mathbf{r}_{bec}$	vector of dimension $3 \times 1$ of tracker beacon position relative aircraft center of gravity in aircraft body axes, ft
$\mathbf{r}_{ILS}$	vector of dimension $3 \times 1$ of ILS antenna position relative aircraft center of gravity in aircraft body axes, ft
$\mathbf{T}_{RB}$	transformation matrix of dimension $3 \times 3$ to transform a vector in aircraft body axes ( $X_B, Y_B, Z_B$ ) to fixed runway axes (see eq. (6))
$\eta_{deg}$	ILS receiver localizer deviation measurement, deg
$\eta_{ILS}$	ILS receiver localizer deviation measurement, dots
$\eta_{trk}$	ILS localizer deviation from runway centerline computed from tracking data, deg
$\theta$	pitch attitude of aircraft, rad
$\phi$	roll attitude of aircraft, rad
$\psi$	yaw rotation angle, rad (see eq. (3))

$\Delta\psi$	aircraft heading relative to runway heading, $\psi_T - \psi_{rw}$ , rad
$\psi_N$	direction of line with respect to true north, deg (appendix B)
$\psi_T$	true heading of aircraft with respect to true north, deg
$\psi_{rw}$	true heading of runway with respect to true north, rad

## Description of Test Equipment

The equipment used for the flight test consisted of a test airplane with a Differential Global Position System (DGPS) for accurate navigation and an on-board real-time data recording system, a radar tracker with a real-time data recording system located 720 ft to the left and approximately halfway down runway 25L, and the ILS system located on a parallel runway 25L at LAX. (See fig. 1.)

### Test Airplane

The airplane used for this flight test was the Transport Systems Research Vehicle (TSRV), which is a modified Boeing 737-100 airplane operated by Langley Research Center (fig. 2). The TSRV is a flying laboratory used for research purposes. It is equipped with highly flexible experimental systems including an electronic flight display system, a digital fly-by-wire flight control and flight guidance system, a side stick controller, and an advanced area navigation system. These experimental systems have been overlaid on the conventional airplane navigation and flight control systems.

Flight operations during this test were performed in the research flight deck (RFD), which is located in the cabin behind the conventional flight deck as shown in the cutaway model of the airplane in figure 3. The interior of the RFD (fig. 4) is a full-size flight deck that contains eight 8- by 8-in. flight-quality, color CRT displays. Each RFD pilot has a primary flight display and a navigation display. The four CRT's on the center panel of the flight deck are used for engine instruments, check lists, and flight test purposes.

Selection of flight control and flight guidance modes during test flights may be chosen by the flight crew through the mode control panel (MCP) located in the center of the glare shield. Three-dimensional flight paths, including preprogrammed flight routes, may be programmed through the navigation control display unit (CDU) located next to each pilot's knees. These paths are displayed on the navigation display

(ND), located just above the CDU, and guidance is provided on this display and the primary flight display (PFD) just above the navigation display.

A DGPS system (ref. 1) was used to compute accurate position estimates onboard the airplane during these tests (approximately 30 ft with  $2\sigma$  position accuracy). The accuracy of the estimates for these tests was an order of magnitude better than the best current aircraft navigation systems. The accurate navigation allowed the TSRV to repeatably fly on the same path in space so that a consistent set of data was provided for modeling the ILS localizer.

The TSRV used the DGPS estimates only for horizontal path guidance. Because GPS vertical accuracy is at times much less accurate than barometric altimetry, vertical path guidance was derived from corrected barometric altimeter measurements.

### FAA RIR-778X Radar Tracker

The radar used during this test is an X-band, RIR-778X radar tracker (fig. 5). This tracking system is totally portable and was operated by the FAA Technical Center, Atlantic City, NJ.

The radar was designed to constantly track and determine the position of a target in real time. The user may select either RF or optically derived data. During this test, an automatic RF tracking mode was used. This mode was enhanced with the use of a transponder located in the airplane and a transponder beacon mounted on the aft underbelly of the airplane.

The radar tracker provided filtered, time-tagged Cartesian position and velocity data printed in an alphanumeric form. Ground track and altitude plots were also provided after each flight. Data were recorded on a magnetic tape drive at 10 times/sec for postflight merging with the data recorded in the airplane.

The vertical and lateral angular accuracy of the RIR-778X radar tracker is 0.1 mrad rms. (At a distance of 8 n.mi. from the antenna, this is equivalent to 4.9 ft; at 30 n.mi., 18.2 ft.) Range accuracy is specified as 10 ft rms at a range of 25 n.mi.

### ILS System

The ILS system observed for these flight tests provides approach and landing guidance to runway 25L at Los Angeles International Airport. The localizer system utilizes dual transmitters and frequencies for increased accuracy. The localizer signal is utilized for an ATC navigation reference point more than 52 n.mi. from the localizer antenna. This

ILS system is certified for Category II approach procedures.

The localizer output signal was recorded by the TSRV data recording system and was also used to drive a localizer deviation indicator on the RFD displays of the TSRV. The indicator is used by the pilot to fly the airplane manually or to monitor automatically controlled flight. The indicator shows the pilot the horizontal angular deviations from the localizer centerline (intended to overlay the runway centerline). Full-scale deflections on the indicator are equivalent to  $\pm 150 \mu\text{A ddm}$ . The indicator has two equally spaced dots on both sides of the zero deflection mark and a deflection at the second dot is equivalent to  $150 \mu\text{A ddm}$ .

ILS installations are calibrated to produce  $150 \mu\text{A ddm}$  at the ILS receiver localizer output when it is located 350 ft off the runway centerline at runway threshold. For the ILS installation on runway 25L at LAX the  $150 \mu\text{A ddm}$  (indicator full-scale deflection of 2 dots) corresponds to an angle of  $1.67^\circ$  from localizer centerline.

## Test Design

### Technical Approach

The technical approach used to determine the location and contour of the ILS localizer was to compare the radar-tracker-measured path of the TSRV ("truth position") with the localizer receiver output recorded and UTC time-tagged on the TSRV. The measured truth position of the TSRV was also UTC time-tagged and recorded by the radar tracker system while the airplane was precisely flown by the TSRV automatic flight control system on two flight test paths. The comparison process consisted of merging the recorded data, computing an equivalent ILS localizer deviation using the truth position, and computing the differences between the measured and computed localizer deviations. The computed differences were then plotted and statistically analyzed.

The analysis was performed on data recorded for an ascending flight segment above the extended runway centerline and on path segments perpendicular to the extended runway centerline in the range of 10 to 32 n.mi. from the localizer antenna. (See fig. 6.)

### Flight Paths

Two serpentine-shaped flight test paths (called northerly and southerly paths with southerly shown in fig. 7) were flown to position the aircraft along the desired flight segments shown in figure 6. The

navigation system used the stored flight paths to compute guidance that was displayed on the RFD displays and coupled to the automatic flight control system. Each flight path was alternately flown by the automatic flight control system.

Each path contained straight-leg segments perpendicular to the runway centerline, flown left to right and right to left. The perpendicular segments were equally spaced 2 n.mi. apart at distances from 10 n.mi. to 32 n.mi. from the localizer antenna. The altitudes of these segments were set equal to the altitude of the glide slope at their localizer crossing points. The length of each segment was 3.3 n.mi. long to ensure that potential localizer beam distortion and ILS localizer offsets at extended runway centerline distances did not result in the desired portions of the localizer signal being unrecorded.

The perpendicular straight-leg segments were connected with  $180^\circ$  turn segments that had a constant radius of 2 n.mi. Altitude changes from one straight-leg segment to the next were made during the turns. (See altitude profile at bottom of fig. 7.)

The two paths were mirror images of each other; this resulted in the direction of flight on the respective perpendicular segments being in opposite directions. The use of the mirrored paths provided a means to identify and null any time-synchronization errors between the airborne and ground data.

The southerly trajectory begins at the perpendicular segment located 32 n.mi. from the localizer antenna (segment labeled AB in fig. 7). The trajectory progresses towards the runway on perpendicular segments 4 n.mi. apart. At the end of the perpendicular segment 12 n.mi. from the antenna (labeled CD in fig. 7), the trajectory continues with a  $270^\circ$  turn ending directly above the runway centerline at point E and proceeds up the glide slope away from the runway. At 32 n.mi. away from the localizer antenna, the trajectory then continues with another  $270^\circ$  turn onto the perpendicular segment FG (fig. 7). Then it again progresses toward the runway traversing every other perpendicular segment (those not crossed during the first progression toward the runway). At the end of the segment labeled HI in figure 7, the trajectory continues with another  $270^\circ$  turn onto the runway centerline that again proceeds approximately up the glide slope away from the runway. The trajectory ends at 34 n.mi. away from the localizer antenna (point J in fig. 7). When the glide slope reaches 10 000 ft, the altitude profile remains level.

The airspace required to fly these paths consisted of a block 4 n.mi. wide on each side of the extended



Table 1. Surveyed Data Points Using WGS-84 Earth Model

Surveyed point	Latitude, deg	Longitude, deg	$h_{MSL}$ , ft	Height above WGS-84 reference ellipsoid, ft
<b>ILSE</b>	33.933483342	-118.422077122	118.0	0.83
<b>R07R</b>	33.939552392	-118.382904500	95.3	-21.87
<b>R25L</b>	33.937508653	-118.382729694	96.2	-20.95
<b>NASA</b>	33.938241242	-118.416833908	157.9	40.77
<b>SPIKE</b>	33.933948810	-118.398090403	111.8	-5.31
<b>NIKE</b>	33.933342544	-118.404013506	116.3	-0.87
<b>MERC</b>	33.938762928	-118.417807133	117.5	0.37

runway centerline (total 8 n.mi. wide, fig. 8), between 34 n.mi. and 6 n.mi. from the localizer antenna, and between 10 000 ft MSL and 2500 ft MSL. A complete waypoint description for these paths is given in appendix A in terms of latitude, longitude, mean-sea-level altitude, and  $x, y, z$  coordinates of a fixed runway coordinate system.

**Runway Coordinate System ( $x_{rw}, y_{rw}, z_{rw}$ )**

A fixed runway coordinate system was defined to facilitate computation of an equivalent ILS localizer deviation from the radar measurement. (See fig. 9.) Its origin was located at the ILS localizer antenna on the extended runway centerline for runway 25L (at surveyed point **ILSE**). The  $X_{rw}$ -axis lies along the runway centerline pointing opposite to the direction of landing. The  $Z_{rw}$ -axis points upward and the  $Y_{rw}$ -axis points in a direction that completes a right-handed coordinate frame.

Table 1 defines the seven surveyed points (determined to an accuracy  $\pm 1$  mm) that were used to define the runway coordinate system and to perform preflight operational checks of the TSRV DGPS navigation system. Since the DGPS navigation system operates in the WGS-84 coordinate system (World Geodetic System 1984, ref. 2), all surveyed points were specified in that system. The surveyed points are as follows:

- ILSE** location of runway coordinate system origin
- R07R, R25L** runway threshold points on runway centerline
- NASA** location of DGPS ground station
- SPIKE** flight calibration point
- NIKE** location of radar tracker
- MERC** preflight calibration point

The direction of the  $X_{rw}$ -axis of the runway coordinate system relative to true north (designated  $\psi_N$  on fig. 9) was computed to be  $82.991985^\circ$  from true north. The equations used to compute the direction are given in appendix B.

The position vectors, the aircraft body axes system, and the table at the bottom of figure 9 are discussed in the section "Data Analysis."

**Recorded Data**

The recorded data for these tests were obtained during flight tests on three consecutive days—April 1, 2, and 3, 1992. The data were gathered during the early morning hours of the day from approximately 12 p.m. to 5 a.m. since the unusual test paths could not be flown during normal LAX daytime operations.

The airborne parameters recorded on magnetic tape for use in postflight analysis were time, the ILS receiver output in units of dots, and aircraft attitude and true heading in degrees. These data were recorded at 20 times/sec.

On the ground the radar tracker recorded time and the position of a radar beacon mounted on the TSRV aft underbelly surface. The TSRV beacon position, was recorded in terms of azimuth, elevation, and range relative to the radar tracker surveyed site at 10 times/sec. After the test flights, the beacon position was translated into the fixed runway coordinate system described in the previous section.

**Data Analysis**

The location of the ILS localizer centerline relative to runway 25L centerline and the localizer contour were determined by analysis of differences between the recorded localizer deviation output from the ILS receiver ( $\eta_{ILS}$ ) and an equivalent localizer deviation (or truth signal  $\eta_{trk}$ ) computed from the

airplane position recorded by the radar tracker. Note that the output from the ILS receiver represented the deviation of the airplane ILS localizer antenna from the ILS localizer beam centerline, whereas the equivalent localizer deviation represented the airplane localizer antenna deviation from runway centerline.

After the differences between the equivalent and ILS receiver localizer deviations were computed, scatter plots of differences versus the equivalent localizer deviation were made. Curves were then fit to these scatter plots to characterize the location and contour of the ILS receiver localizer deviations.

### Merging Tracker and Aircraft Data

The first step in data merging was to convert the ground-based tracking data from 10 samples/sec to 20 samples/sec. This conversion was done to match the airborne data tapes recorded at 20 samples/sec. The additional tracking data points and any missing data points were determined by linear interpolation. The new ground-based tracking data tape and the airborne data tape were then merged. The airborne data tape time stamps were used as a reference to synchronize the ground-based tracking tape.

**Corrections for ILS and transponder antenna locations.** The localizer receiver deviation data were relative to the ILS localizer antenna located on the top of the vertical stabilizer of the TSRV. As noted, the tracker position was relative to the radar beacon antenna on the TSRV. The position difference of these antennas is approximately 36 ft and would introduce significant errors into the data analysis if not taken into account. Thus, the radar tracking position data were translated to the localizer receiver antenna position so that an equivalent localizer deviation could be computed. The translation was accomplished by vector algebra addition.

The vectors for the locations of the ILS antenna  $\mathbf{r}_{ILS}$  (fig. 9), and for the transponder beacon antenna  $\mathbf{r}_{bec}$  were defined within an aircraft body axis<sup>2</sup> system attached to the aircraft. These vectors were transformed to the fixed runway coordinate frame by premultiplication with the transformation matrix  $\mathbf{T}_{RB}$  (derived below). The transformed vectors were summed with the radar tracking data vector  $\mathbf{r}_B$  (which was defined in the runway coordinate frame) to produce the position vector  $\mathbf{r}_A$ , the truth position of the ILS localizer antenna in fixed runway coordinates. The equation for computing the vector  $\mathbf{r}_A$  is given as

$$\mathbf{r}_A = \mathbf{r}_B + \mathbf{T}_{RB}(\mathbf{r}_{ILS} - \mathbf{r}_{bec}) \quad (1)$$

where

$$\mathbf{r}_A = \begin{bmatrix} x_A \\ y_A \\ z_A \end{bmatrix} \quad (2)$$

and  $\mathbf{T}_{RB}$  is derived next.

The transformation matrix  $\mathbf{T}_{VB}$  for transforming a vector from the body axes to the vehicle axes (a fixed axis system with the  $X$ -axis pointing east,  $Y$ -axis pointing north, and  $Z$ -axis pointing down) is defined as

$$\mathbf{T}_{VB} = \begin{bmatrix} \cos \theta \cos \psi & \sin \phi \sin \theta \cos \psi - \cos \phi \sin \psi & \cos \phi \sin \theta \cos \psi + \sin \phi \sin \psi \\ \cos \theta \sin \psi & \sin \phi \sin \theta \sin \psi + \cos \phi \cos \psi & \cos \phi \sin \theta \sin \psi - \sin \phi \cos \psi \\ -\sin \theta & \sin \phi \cos \theta & \cos \phi \cos \theta \end{bmatrix} \quad (3)$$

where  $\phi$ ,  $\theta$ , and  $\psi$  are the pitch, roll, and yaw rotation angles. The  $Z_{rw}$ -axis of the runway coordinate system points up, whereas the vehicle  $Z$ -axis points down. Rotating the vehicle coordinate system about the  $Y$ -axis

---

<sup>2</sup>The aircraft body axes are a coordinate system fixed to the airplane with the origin at the center of gravity, the positive  $X_B$ -axis through the nose, the positive  $Y_B$ -axis through the right wing, and the positive  $Z_B$ -axis pointing downward through the belly of the airplane.

by  $180^\circ$  results in the  $Z$ -axis pointing up and the  $X$ -axis pointing in the direction of the  $X_{rw}$ -axis. The matrix  $\mathbf{T}_y$  which rotates a vector about the  $Y$ -axis by an angle of  $\omega$  is given as

$$\mathbf{T}_y = \begin{bmatrix} \cos \omega & 0 & -\sin \omega \\ 0 & 1 & 0 \\ \sin \omega & 0 & \cos \omega \end{bmatrix} \quad (4)$$

Premultiplying  $\mathbf{T}_{VB}$  by  $\mathbf{T}_y$  with  $\omega = 180^\circ$  results in the transformation matrix  $\mathbf{T}_{RB}$  for translating vectors from the body axes to the runway coordinate system or

$$\mathbf{T}_{RB} = \mathbf{T}_y \mathbf{T}_{VB} \quad (5)$$

If  $\Delta\psi$  is substituted for  $\psi$  in equation (5) for  $\mathbf{T}_{VB}$ , then

$$\mathbf{T}_{RB} = \begin{bmatrix} -\cos \theta \cos \Delta\psi & -\sin \phi \sin \theta \cos \Delta\psi + \cos \phi \sin \Delta\psi & -\cos \phi \sin \theta \cos \Delta\psi - \sin \phi \sin \Delta\psi \\ \cos \theta \sin \Delta\psi & \sin \phi \sin \theta \sin \Delta\psi + \cos \phi \cos \Delta\psi & \cos \phi \sin \theta \sin \Delta\psi - \sin \phi \cos \Delta\psi \\ \sin \theta & -\sin \phi \cos \theta & -\cos \phi \cos \theta \end{bmatrix} \quad (6)$$

where

$$\Delta\psi = \psi_T - \psi_{rw} \quad (7)$$

and  $\theta$ ,  $\phi$ , and  $\psi_T$  are, respectively, the airplane pitch attitude, roll attitude, and true heading with respect to true north. These parameters are measured from the laser gyro inertial strapdown system on the airplane. The true heading of the runway is denoted by  $\psi_{rw}$  and is computed as the runway  $X$ -axis rotation from true north plus  $180^\circ$ . The true heading of the airplane with respect to the runway heading is represented by  $\Delta\psi$ .

**Computation of equivalent localizer deviation.** The radar tracking data vector components (eq. (2)) were used to compute the equivalent localizer deviation ( $\eta_{\text{trk}}$ ) for comparison with the localizer deviation output from the ILS receiver. The equivalent localizer deviation was defined as the angle formed at the origin of the runway coordinate system by the lateral offset of the localizer antenna on the TSRV from the runway centerline. This angle was computed from the components of equation (2) as

$$\eta_{\text{trk}} = \left( \sin^{-1} \frac{-y_A}{|r_A|} \right) \frac{180}{\pi} \text{ deg} \quad (8)$$

**Conversion of recorded localizer deviation from units of dots to degrees.** The localizer deviation output from the ILS receiver was recorded in units of dots deviation from the localizer centerline. Therefore, for comparison with computed localizer deviation from equation (8), this recorded data had to be converted into units of degrees.

The conversion was accomplished with a constant multiplication factor  $f$ , which is a function of the localizer antenna distance from the runway threshold as defined by ILS installation procedures. As described earlier, the ILS localizer beam is adjusted so that an ILS receiver will output  $150 \mu\text{A}$  (equivalent to 2 dots full-scale deviation) when located 350 ft from the runway centerline at the runway threshold (ref. 3). Therefore the conversion factor  $f$  was computed as

$$f = \left( \frac{1}{2} \right) \left( \tan^{-1} \frac{350}{\text{Distance from localizer to threshold}} \right) \frac{180}{\pi} \quad (9)$$

For runway 25L at LAX, the distance from the localizer to the threshold was calculated from the surveyed data to be 12024.7 ft, which resulted in a value for  $f$  of 0.83361 deg/dot. Given  $f$  and the localizer deviation output from the ILS receiver in dots  $\eta_{ILS}$ , the localizer deviation in degrees  $\eta_{deg}$  is

$$\eta_{deg} = f\eta_{ILS} \quad (10)$$

**Computation of differences between localizer deviations.** The difference between the ILS receiver localizer deviation converted to units of degrees and the equivalent localizer deviation was defined as

$$d_{loc} = \eta_{deg} - \eta_{trk} \quad (11)$$

These differences were then analyzed to determine localizer beam centerline relative to runway centerline and to determine the contour of the ILS localizer beam.

### Merged Data Analysis

The computed differences were split into two portions, and each portion was analyzed independently. One portion was for flight along the extended runway centerline, and the other portion was for flight along path segments perpendicular to the extended runway centerline. The computed differences (from eq. (11)) for the portion along the perpendicular path segments were further partitioned into groups corresponding to each of the perpendicular path segments (10 to 32 n.mi. in 2 n.mi. increments).

All differences were computed and stored at 0.5-sec intervals only when the airplane was between the full-scale deviation of the computed localizer signal ( $\pm 1.67^\circ$ ).

**Analysis of data on perpendicular flight segments.** An equal number of computed differences ( $d_{loc}$  from eq. (11)) were used for each direction flown on the perpendicular legs in the data analysis. Scatter plots of the differences versus the computed localizer deviation  $\eta_{trk}$  were made for each of the data group associated with the perpendicular path segments. Linear curve fits were then computed and plotted on each of the scatter plots. All the linear curve fits are of the form

$$d_{cfp} = b + m\eta_{trk} \quad (12)$$

where  $b$  is a constant and  $m$  is the slope of the curve fit. The slope represents a measure of the proportionality of actual localizer deviation to equivalent localizer deviation ( $\eta_{trk}$ ). In other words, equation (12)

gives the angular bias error in the localizer measurement as a function of true angular deviation from runway centerline.

### Analysis of data along runway centerline.

The mean and standard deviation of the differences for localizer centerline flight were computed. A scatter plot of these data was made to observe beam bends. A linear curve fit was also computed with these data for comparison with the perpendicular path data.

## Results

### Perpendicular Flight Segments

Figure 10(a) is a plot of computed differences ( $d_{loc}$ ) as a function of the equivalent localizer deviation ( $\eta_{trk}$ ) for the perpendicular path segment located 10 n.mi. from the localizer antenna. This figure shows that the differences are separated into two groups. One group contains the differences computed from data recorded when the airplane was flown in the northerly direction and the other group contains the differences when the airplane was flown in the southerly direction. The separation indicates that the recorded localizer deviation output from the ILS receiver is older than its associated UTC time-tag on the order of 70 msec—effectively a 70-msec transport delay in recording this output. This transport delay was known to exist, but its value was difficult to determine and led to flying the path segments in both directions so that the delay could be removed by averaging. The recorded radar tracking data matches its UTC time-tag very accurately (to less than 1 msec). The transport delay results in a positive contribution to the computed differences when the localizer is crossed in the positive  $y_{rw}$  direction (northerly) and a negative contribution when crossed in the negative  $y_{rw}$  direction (southerly).

A linear regression curve fit was applied to the data in figure 10(a) and is shown in the plot as a dashed line between the two data groups. The equation for the curve fit (viz, eq. (12) with  $b = -0.079$  and  $m = 0.12905$ ) is shown in the plot. The location of the curve fit (dashed line) on the plot shows that the curve fit averaged out the transport delay in the two data groups.

Figures 10(b) through (l) are plots corresponding to figure 10(a) for perpendicular path ranges of 12, 14, 16, 18, 20, 22, 24, 26, 28, 30, and 32 n.mi. from the localizer antenna. These plots showed that as the range increased, each of the groups of data moved closer to each other. The reason these groups moved closer is that the angular error due to a constant transport delay decreases with increasing distance from the localizer antenna for an airplane flying at constant speed.

The coefficients ( $b$  and  $m$ ) in the linear curves computed for each perpendicular path segment were very close to the same value for all ranges. The constant term  $b$  ranged from  $-0.082^\circ$  to  $-0.078^\circ$  and the slope coefficient  $m$  ranged from 0.13208 and 0.12805. Averaging each of these coefficients results in a general characterization of the computed difference as

$$d_{cfp} = -0.080 + 0.130\eta_{trk} \quad \text{deg} \quad (13)$$

Therefore, based on this analysis of the LAX experimental data, equation (13) is established as a suitable sensor error model for a Category II ILS localizer.

The localizer beam centerline relative to the runway centerline may be found from an equation expressing the localizer deviation from beam centerline ( $\eta_{deg}$ ) as a function of equivalent localizer deviation ( $\eta_{trk}$ ). This equation is formed by substituting  $d_{loc}$  from equation (11) for  $d_{cfp}$  into equation (13); this results in the equation

$$\eta_{deg} = -0.080 + 1.130\eta_{trk} \quad (14)$$

By setting  $\eta_{deg}$  to zero, the ILS beam angular offset from the runway centerline is determined. This results in a localizer beam centerline  $0.071^\circ$  to the left of the runway centerline. The value  $0.071^\circ$  represents a positional offset from true runway centerline of 75 ft at 10 n.mi. and 241 ft at 32 n.mi., which would seem to provide good position accuracy for parallel runway operations.

### Runway Centerline Flight

Figure 11 shows a scatter plot of computed differences as a function of range from the localizer antenna when the airplane was flown on the localizer centerline from 10 to 32 n.mi. from the localizer antenna. These data include a total of 16 passes. The data points above and below the bulk of the data points in the range of 10 to 13 n.mi. resulted from not initially tracking the localizer beam centerline for a couple of runs. Note that  $d_{loc}$  is a function of

how close the aircraft is to the localizer beam centerline. A linear curve fit to these data resulted in the following equation (also shown in fig. 11):

$$d_{cfc} = -0.074 - 0.00007(\text{Range}) \quad (15)$$

This equation represents the ILS localizer centerline offset from the runway centerline as a function of range in units of nautical miles. Substituting 10 n.mi. for range in the equation gives an offset of  $-0.075^\circ$  (left of runway centerline) and substituting 30 n.mi. gives an offset of  $-0.076^\circ$ . Equation (15) shows that the localizer centerline offset from the runway centerline is essentially constant with range.

The data in figure 11 shows that ILS localizer beam did not contain any significant beam bends. Two very small beam bends are shown by the two slight dips in the data that reach a minimum offset at around 12 and 20 n.mi. from the ILS antenna. From observation of the data, the dips deviate from the average offset by approximately  $0.01^\circ$ .

The mean and standard deviation of the centerline data were computed to be, respectively,  $-0.075^\circ$  and  $0.011^\circ$ . The value of the standard deviation is suitable for use in modeling the noise on the localizer measurement.

### Localizer Contour

Figure 12 shows one of the runs crossing the localizer perpendicularly in the northerly direction from figure 10(h) (range equal to 24 n.mi.) with expanded scales. The plot shows that the computation of linear deviation from the localizer is only good to approximately  $\pm 2^\circ$ . The relatively constant slope of the curve between  $\pm 2^\circ$  of deviation represents the linearity and the proportionality of the measured localizer deviation to the true angular deviation from the runway centerline. If the slope was zero, the localizer measurement would represent a true angular measurement relative to the localizer beam centerline. The slope shown is essentially that given in equation (12). This plot is typical of the data for other ranges from the localizer.

### Summary of Results

During a brief FAA/NASA flight test program, instrument landing system (ILS) localizer receiver signals on runway 25L at Los Angeles International Airport and airplane position were recorded and UTC time-tagged at a range 10 to 32 n.mi. from the localizer antenna. The primary purpose for gathering and analyzing these data was for use in modeling the ILS localizer at an extended range

for future simulation studies, particularly on closely spaced parallel runways. A secondary purpose was to document the location of the ILS localizer beam centerline relative to the runway centerline for future airplane tracking tests.

A consistent set of data was obtained for statistical analysis by automatically controlling the airplane to make multiple trips along two preprogrammed flight paths. Differential GPS (Global Positioning System) was used for precision airborne navigation. These flight paths were designed to gather the data in an organized way. Each flight path contained (1) multiple path segments perpendicular to the extended runway centerline (at 2-n.mi. intervals) and (2) a single path segment along the localizer centerline between 10 and 32 n.mi. from the ILS localizer antenna.

A precision ground-based radar was used to measure, time-tag, and record the aircraft position for use as the truth position reference. The airborne and ground data were merged. Differences between the ILS localizer receiver data recorded on the airplane and an equivalent localizer signal calculated from the recorded radar tracker position of the airplane were computed at 0.5-sec intervals and analyzed.

Results of analyzing the differences between the measured ILS receiver localizer deviation and an equivalent localizer deviation, computed from radar tracker aircraft position measurements, are summarized as follows:

1. The ILS localizer centerline was found to be offset  $0.071^\circ$  to the left of the runway centerline based on analysis of the perpendicular path segment data.

2. From analysis of ILS beam centerline tracking data, essentially the same offset was found for ILS localizer centerline. From a curve fit of these data as a function of range, the ILS localizer centerline was found to be located to the left of runway centerline by  $0.075^\circ$  at 10 n.mi. and  $0.076^\circ$  at 30 n.mi.
3. The localizer centerline offset relative to the runway centerline obtained by calculating the mean of the localizer deviation while tracking the runway centerline resulted in a value of  $0.075^\circ$ .
4. No significant beam bends were found in the ILS localizer. Two insignificant beam bends of approximately  $0.01^\circ$  were found at locations 12 and 20 n.mi. from the ILS localizer antenna.
5. The standard deviation of the differences computed from data recorded while tracking the ILS localizer centerline was found to be  $0.011^\circ$ . This value is suitable for use in modeling the noise on the localizer measurement.
6. For simplified modeling purposes, the ILS localizer angular bias error  $d_{loc}$  in degrees can be characterized as

$$d_{loc} = -0.080 + 0.130\eta_{trk}$$

where  $\eta_{trk}$  is the true localizer angular deviation in degrees from runway centerline.

NASA Langley Research Center  
Hampton, VA 23681-0001  
September 20, 1994

## Appendix A

### Path Waypoints

These waypoints define both the northerly and southerly paths. Waypoints to the north of the runway centerline are labeled NORxx. Waypoints to the south of the runway centerline are labeled SOUxx. Waypoints on the runway centerline are labeled CENxx. End of the waypoints defining a turn south of the runway centerline are labeled SSOxx. End of the waypoints defining a turn north of the runway centerline are labeled NNOxx. The xx's at each end of the labels denote the distance between the waypoint and the localizer antenna in nautical miles. The waypoints are given in the following table:

Waypoint	$x_{rw}$ , ft	$y_{rw}$ , ft	$z_{rw}$ , ft	lt, deg	lg, deg	$h_{MSL}$ , ft
SSO10	60761.0	-12152.2	2555.6	33.92054421	-118.21843247	2765.0
SOU10	60761.0	-10155.1	2555.6	33.92599167	-118.21922260	2765.0
NOR10	60761.0	10155.1	2555.6	33.98139093	-118.22726390	2765.0
NNO10	60761.0	12152.2	2555.6	33.98683828	-118.22805516	2765.0
SSO12	72913.2	-12152.2	3186.1	33.92454603	-118.17867701	3434.0
SOU12	72913.2	-10155.1	3186.1	33.92999357	-118.17946463	3434.0
NOR12	72913.2	10155.1	3186.1	33.98539361	-118.18748027	3434.0
NNO12	72913.2	12152.2	3186.1	33.99084104	-118.18826901	3434.0
SOU14	85065.4	-10155.1	3816.6	33.93398237	-118.13970549	4110.0
NOR14	85065.4	10155.1	3816.6	33.98938317	-118.14769547	4110.0
SOU16	97217.6	-10155.1	4447.1	33.93795807	-118.09994524	4793.0
NOR16	97217.6	10155.1	4447.1	33.99335959	-118.10790954	4793.0
SOU18	109369.8	-10155.1	5077.5	33.94192067	-118.06018390	5483.0
NOR18	109369.8	10155.1	5077.5	33.99732289	-118.06812252	5483.0
SOU20	121522.0	-10155.1	5708.0	33.94587016	-118.02042152	6181.0
NOR20	121522.0	10155.1	5708.0	34.00127306	-118.02833445	6181.0
SOU22	133674.2	-10155.1	6338.5	33.94980654	-117.98065813	6885.0
NOR22	133674.2	10155.1	6338.5	34.00521008	-117.98854535	6885.0
SOU24	145826.4	-10155.1	6969.0	33.95372981	-117.94089377	7597.0
NOR24	145826.4	10155.1	6969.0	34.00913397	-117.94875527	7597.0
SOU26	157978.6	-10155.1	7599.5	33.95763996	-117.90112848	8315.0
NOR26	157978.6	10155.1	7599.5	34.01304472	-117.90896428	8315.0
SOU28	170130.8	-10155.1	8230.0	33.96153699	-117.86136230	9041.0
NOR28	170130.8	10155.1	8230.0	34.01694232	-117.86917237	9041.0
SSO30	182283.0	-12152.2	8860.5	33.95997280	-117.82083038	9775.0
SOU30	182283.0	-10155.1	8860.5	33.96542090	-117.82159527	9775.0
NOR30	182283.0	10155.1	8860.5	34.02082677	-117.82937960	9775.0
NNO30	182283.0	12152.2	8860.5	34.02627476	-117.83014558	9775.0
SSO32	194435.2	-12152.2	8976.5	33.96384424	-117.78104933	10000.0
SOU32	194435.2	-10155.1	8977.6	33.96929253	-117.78181173	10000.0
NOR32	194435.2	10155.1	8977.5	34.02470027	-117.78957050	10000.0
NNO32	194435.2	12152.2	8976.4	34.03014846	-117.79033393	10000.0
CEN08	48608.8	0.0	2589.6	33.94967552	-118.26301659	2765.0
CEN10	60761.0	0.0	2557.9	33.95369143	-118.22324197	2765.0
CEN32	194435.2	0.0	8980.0	33.99699652	-117.78568993	10000.0
CEN34	206587.4	0.0	8863.8	34.00085685	-117.74583353	10000.0
SSO08	48608.8	-12152.2	2586.1	33.91652984	-118.25819189	2765.0
NNO08	48608.8	12152.2	2586.1	33.98282084	-118.26784498	2765.0

## Appendix B

### Computation of Direction of Line Relative to True North $\psi_N$

The direction of a line through two points (e.g., waypoints or surveyed points) specified in terms of WGS-84 (ref. 2) coordinates (latitude, longitude, ellipsoid height) can be found from the following equations where one of the points is the apex of the angle between the line and true north.

#### Equations To Transform Point to Earth-Centered, Earth-Fixed (ECEF) Coordinates ( $x_{ec}$ , $y_{ec}$ , $z_{ec}$ )

Given

1. Specification of point in latitude (lt) in degrees, longitude (lg) in degrees, and ellipsoid height ( $h$ ) in feet
2. Flattening (ellipticity) constant,  $f = \frac{1}{298.257223563}$
3. Earth model semimajor axis constant,  $r = 6378137$  m
4. Constant for conversion from degrees to radians,  $rp d = \frac{\pi}{180}$

Then, the equations to compute ECEF coordinates ( $x_{ec}$ ,  $y_{ec}$ ,  $z_{ec}$ ) in units of feet are computed from the following expressions:

$$\begin{aligned} esq &= f(2 - f) \\ a &= r(3.280839895) \\ sp &= \sin[\text{lt}(rp d)] \\ cp &= \cos[\text{lt}(rp d)] \\ sl &= \sin[\text{lg}(rp d)] \\ cl &= \cos[\text{lg}(rp d)] \\ gsq &= 1.0 - [esq(sp)^2] \\ e &= \frac{a}{(gsq)^{1/2}} \\ en &= e - [esq(e)] \\ z' &= (en + h)cp \\ x_{ec} &= z'(cl) \\ y_{ec} &= z'(sl) \\ z_{ec} &= (en + h)sp \end{aligned}$$

#### Equations To Transform ECEF Coordinates to East, North, and Up Coordinates

The equations to compute east, north, and up coordinates ( $x_e$ ,  $y_n$ ,  $z_{up}$ ) given a point specified in ECEF coordinates and the origin specified in both ECEF coordinates and latitude ( $lt_o$ ), longitude ( $lg_o$ ), and ellipsoid height ( $h_o$ ) are given as follows. Let

$$v_p = \begin{bmatrix} x_p \\ y_p \\ z_p \end{bmatrix}$$



which is a point in ECEF coordinates, and

$$v_o = \begin{bmatrix} x_o \\ y_o \\ z_o \end{bmatrix}$$

which is the origin in ECEF coordinates. Then

$$d = v_p - v_o$$

$$sla = \sin[lt_o(rpd)]$$

$$cla = \cos[lt_o(rpd)]$$

$$slo = \sin[lg_o(rpd)]$$

$$clo = \cos[lg_o(rpd)]$$

$$T = \begin{bmatrix} -slo & clo & 0 \\ -sla(clo) & -sla(slo) & cla \\ cla(clo) & cla(slo) & sla \end{bmatrix}$$

$$\begin{bmatrix} x_e \\ y_n \\ z_{up} \end{bmatrix} = Td$$

### Equation To Compute Direction of Line Relative to True North $\psi_N$

The equation to compute  $\psi_N$  is

$$\psi_N = \left( \tan^{-1} \frac{x_e}{y_n} \right) \frac{180}{\pi}$$

## References

1. Vallot, Lawrence; Snyder, Scott; Schipper, Brian; Parker, Nigel; and Spitzer, Cary: Design and Flight Test of a Differential GPS/Inertial Navigation System for Approach/Landing Guidance. *Navigation*, vol. 38, no. 2, Summer 1991, pp. 103–122.
2. *Department of Defense World Geodetic System 1984: Its Definition and Relationships With Local Geodetic Systems*. DMA TR 8350.2, Defense Mapping Agency, Sept. 30, 1987. (Available from DTIC as AD A188 815.)
3. Fries, James R.: Improvement of Automatic Landing Through the Use of a Space Diversity ILS Receiving System. *IEEE Trans. Aerosp. & Elect. Syst.*, vol. AES-7, no. 1, Jan. 1971, pp. 47–53.

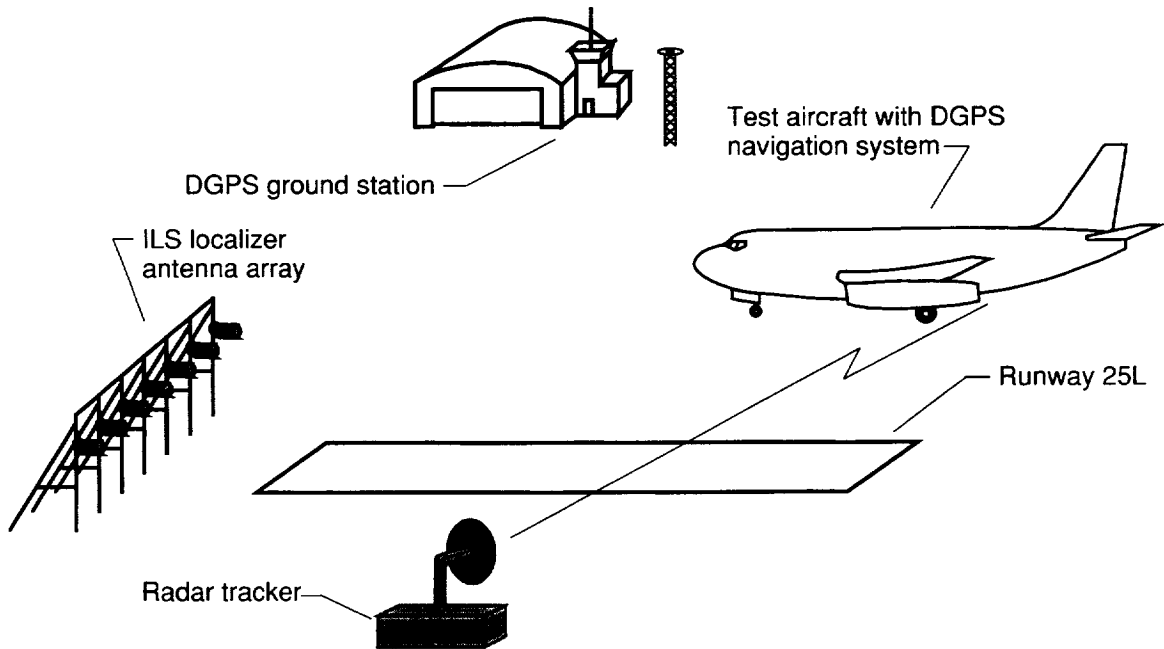


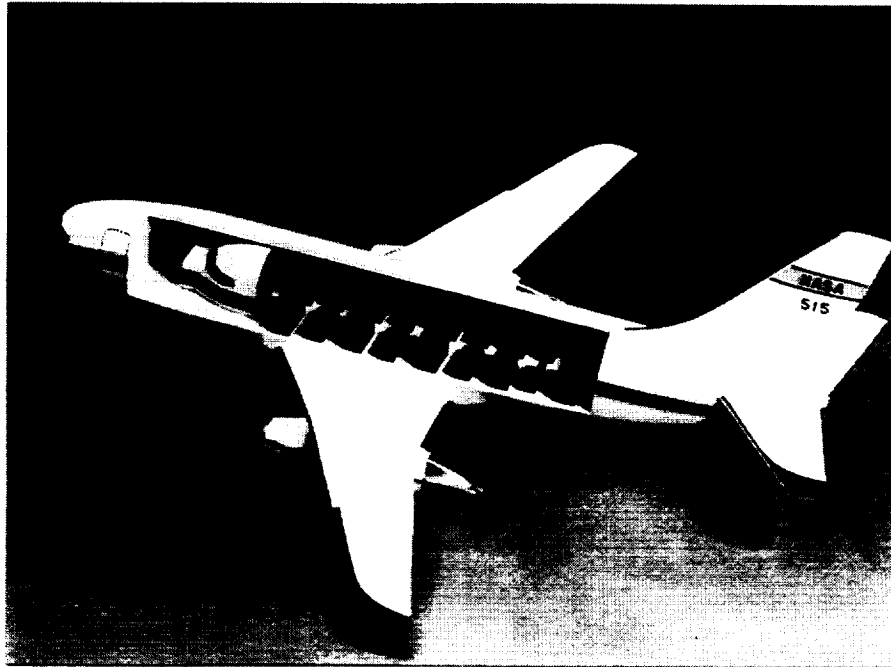
Figure 1. Flight test system components.



L-89-12405

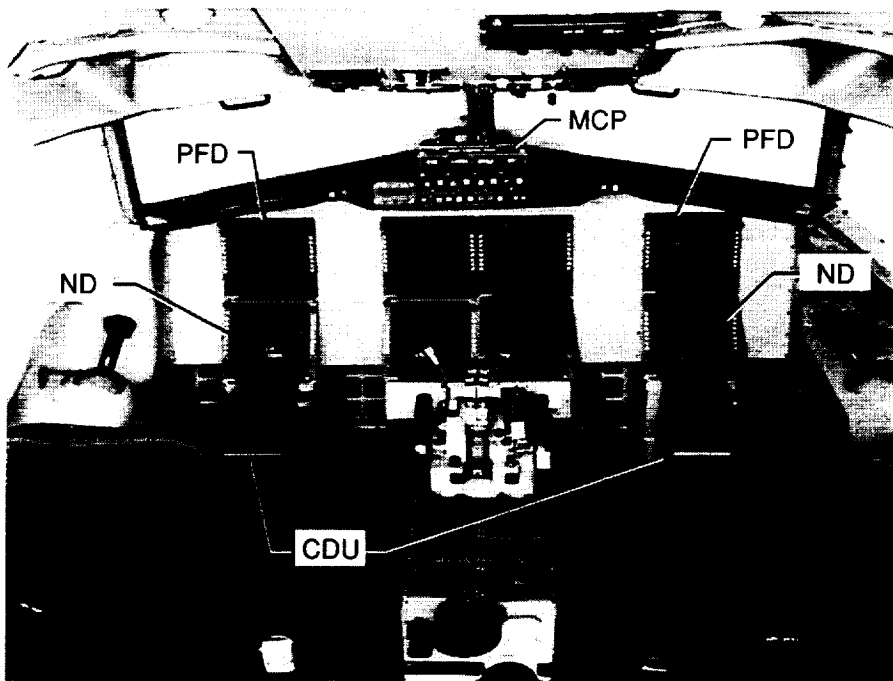
Figure 2. Transport Systems Research Vehicle test airplane.

ORIGINAL PAGE  
BLACK AND WHITE PHOTOGRAPH



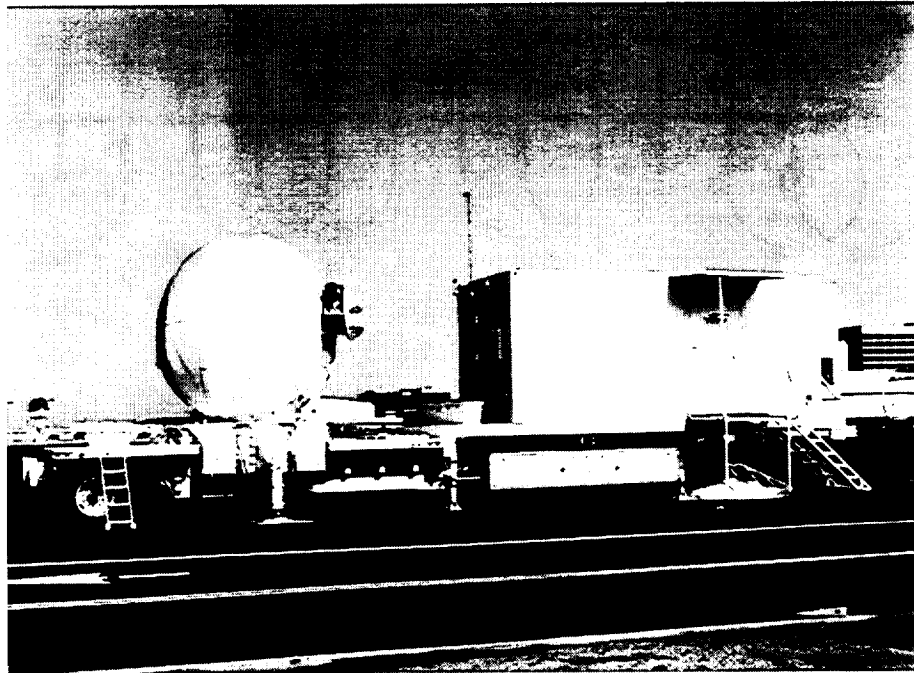
L-80-2580

Figure 3. Model of cabin of Transport Systems Research Vehicle.



L-90-13735

Figure 4. Research flight deck inside Transport Systems Research Vehicle.



L-92-04147

Figure 5. X-band, RIR-778X precision radar tracker.

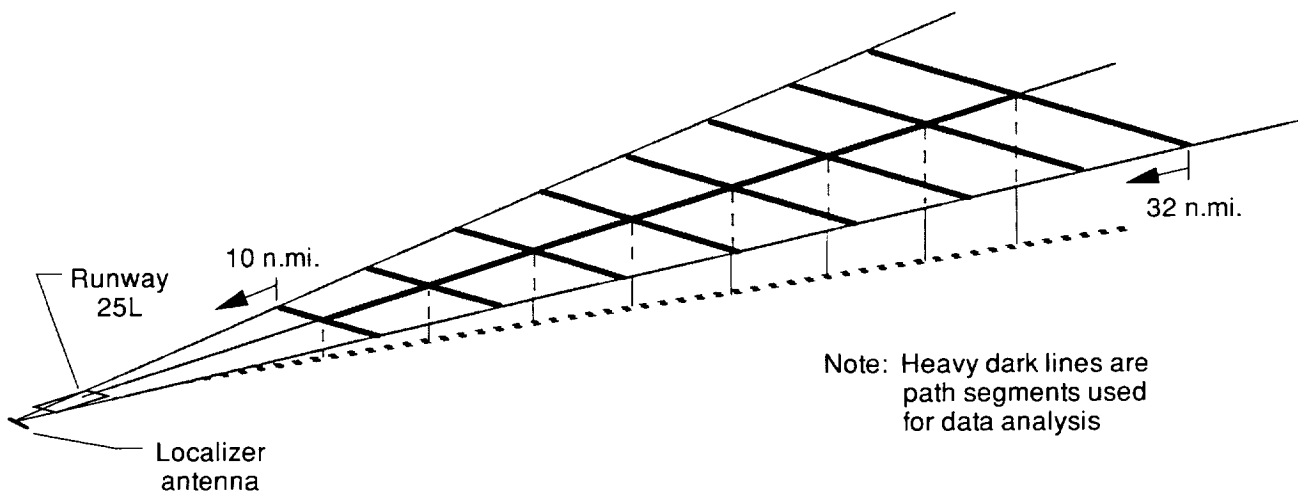


Figure 6. Flight path segments in localizer signal area used for data analysis.

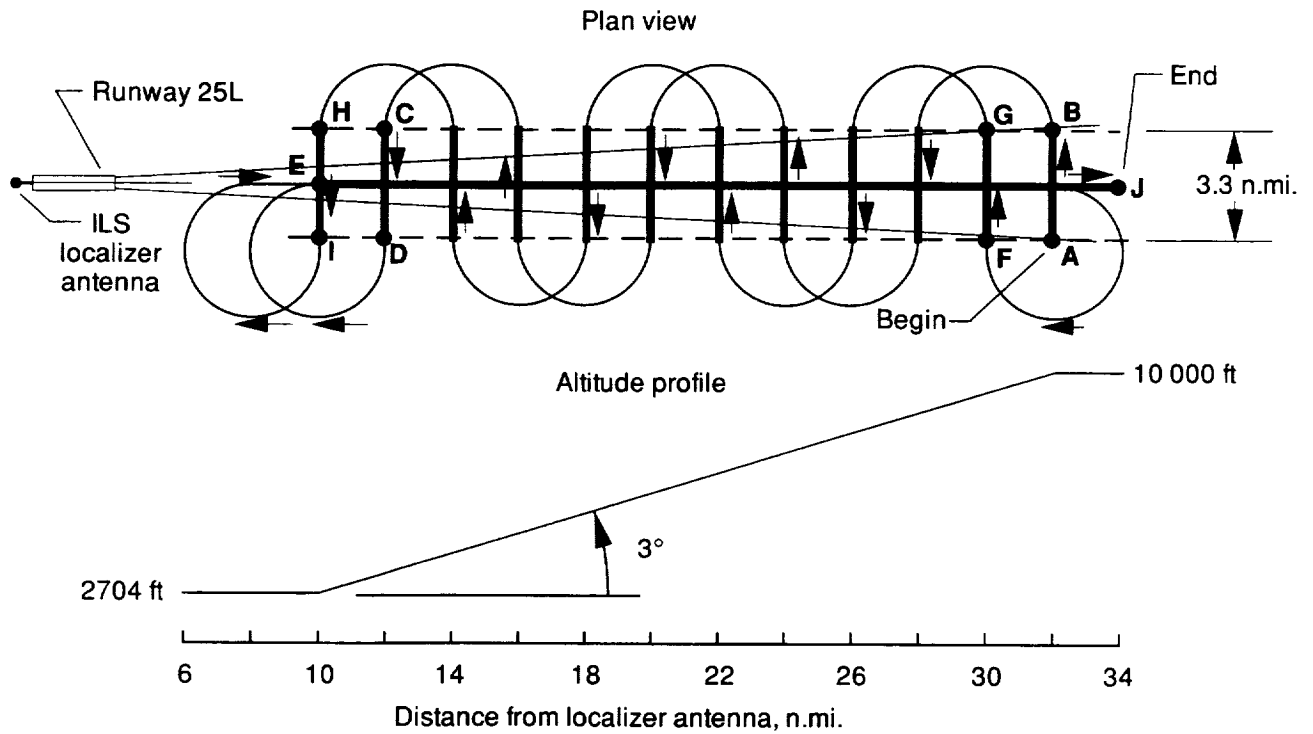


Figure 7. Southerly approach path geometry.

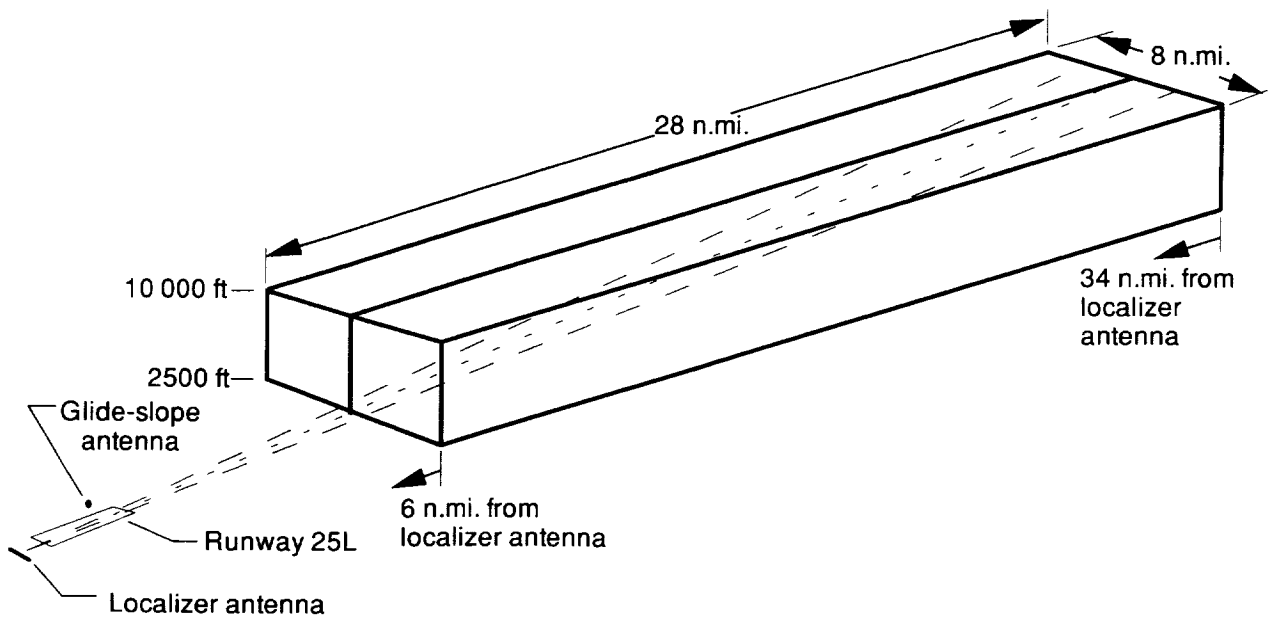


Figure 8. Required airspace for maneuvering on programmed flight paths during data collection flights.

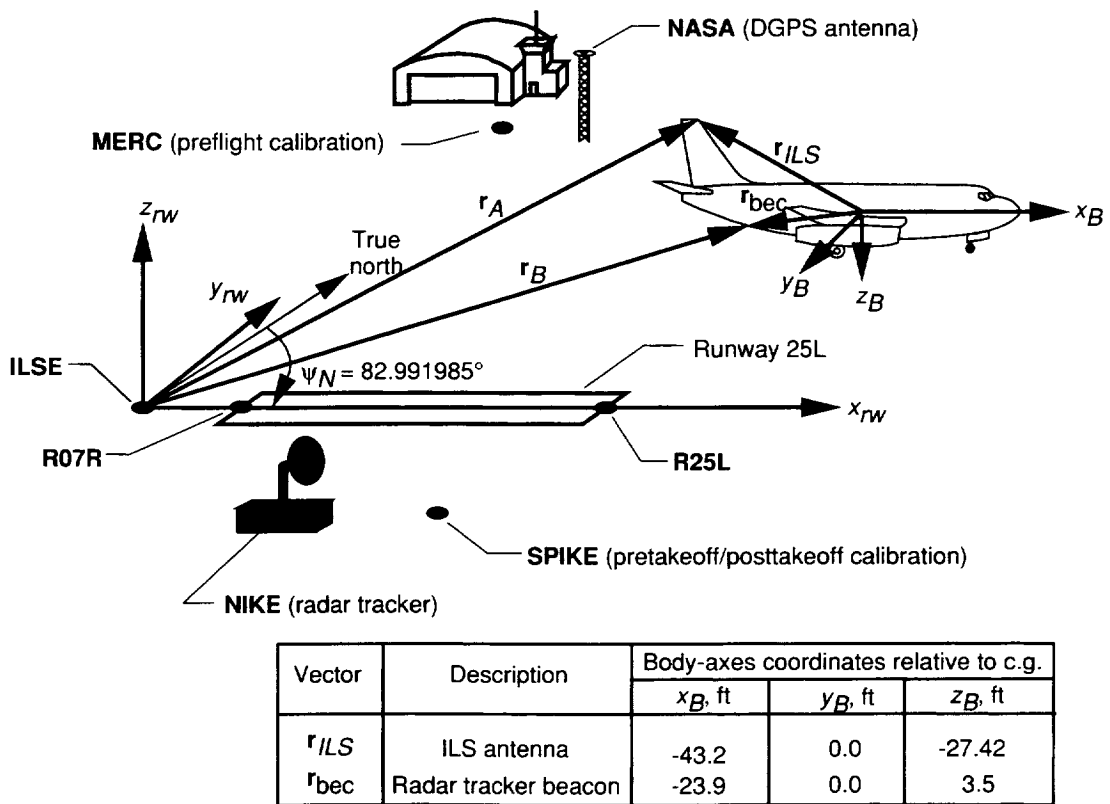
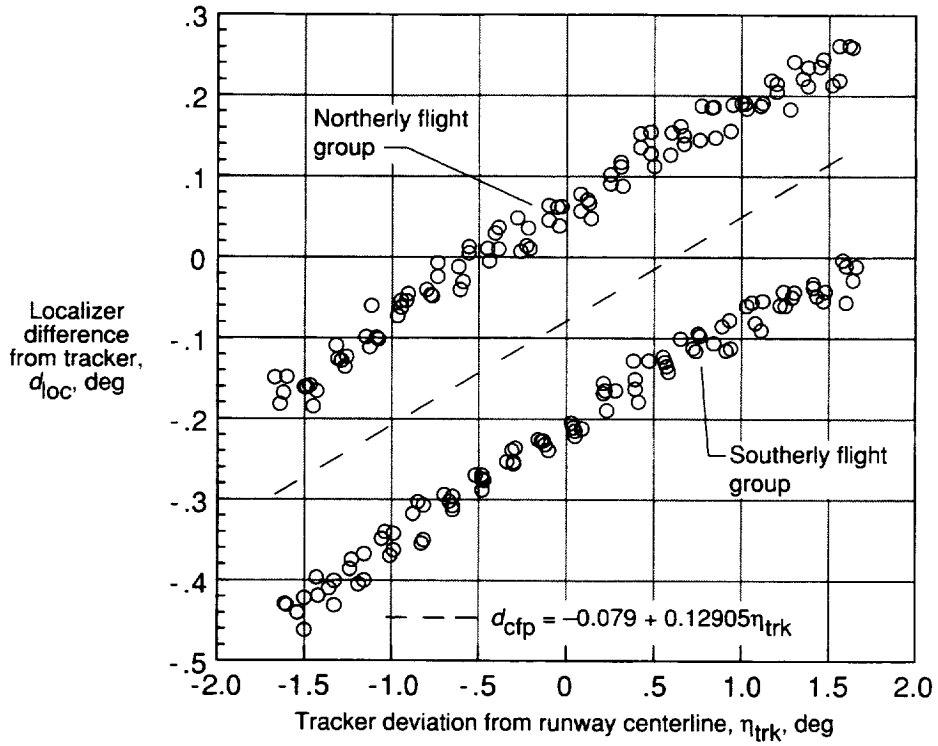
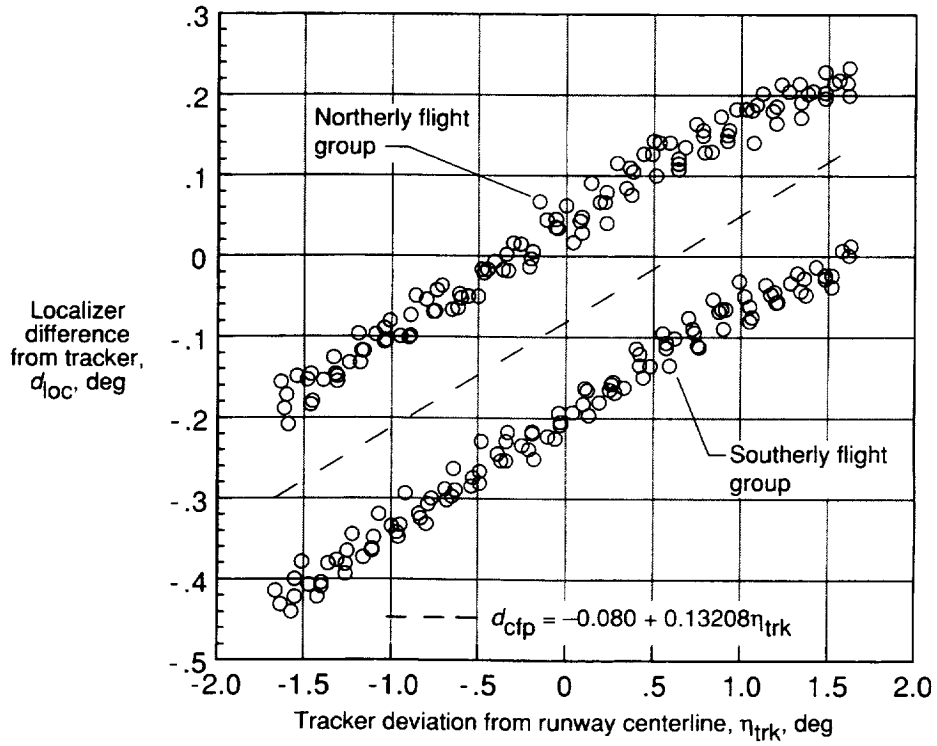


Figure 9. Flight test coordinate system. Surveyed points are in bold type.



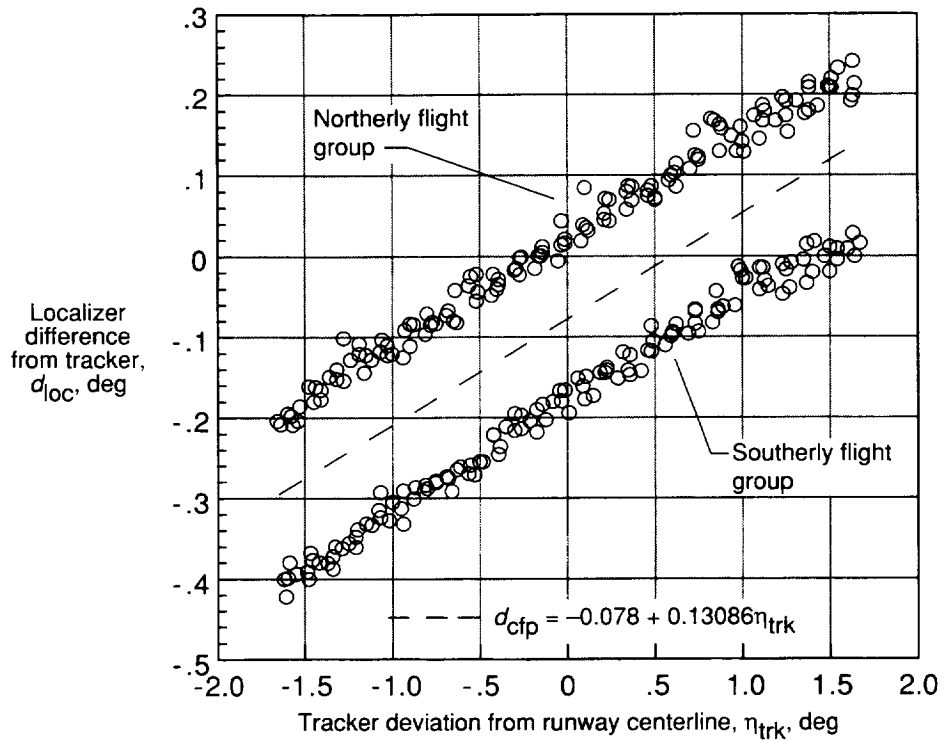
(a) Range of 10 n.mi.



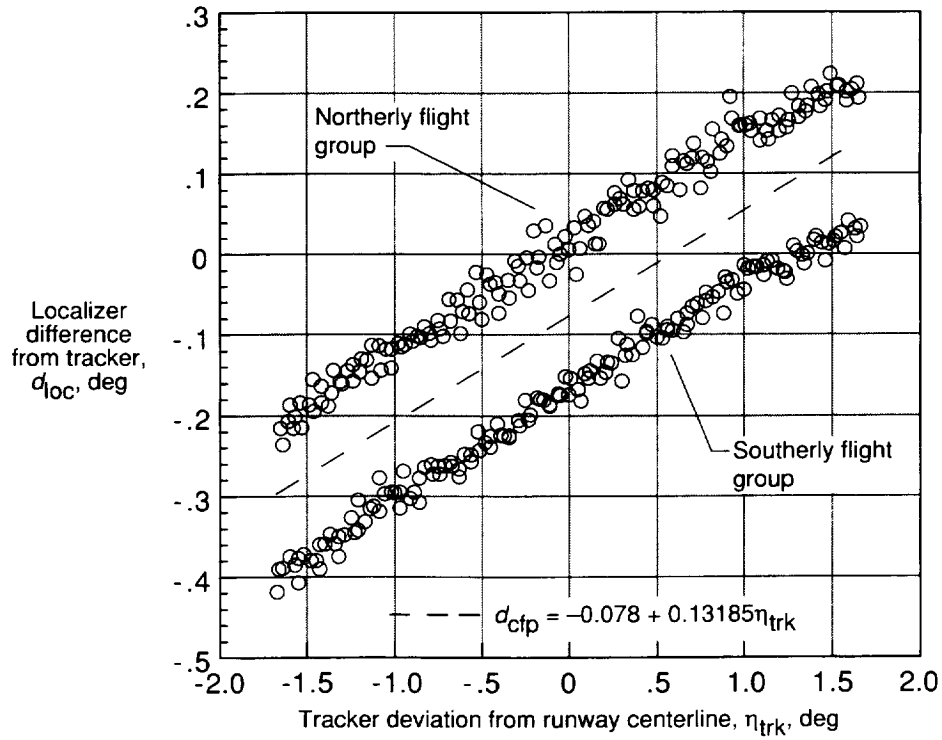
(b) Range of 12 n.mi.

Figure 10. Localizer difference as function of tracker deviation from runway centerline.



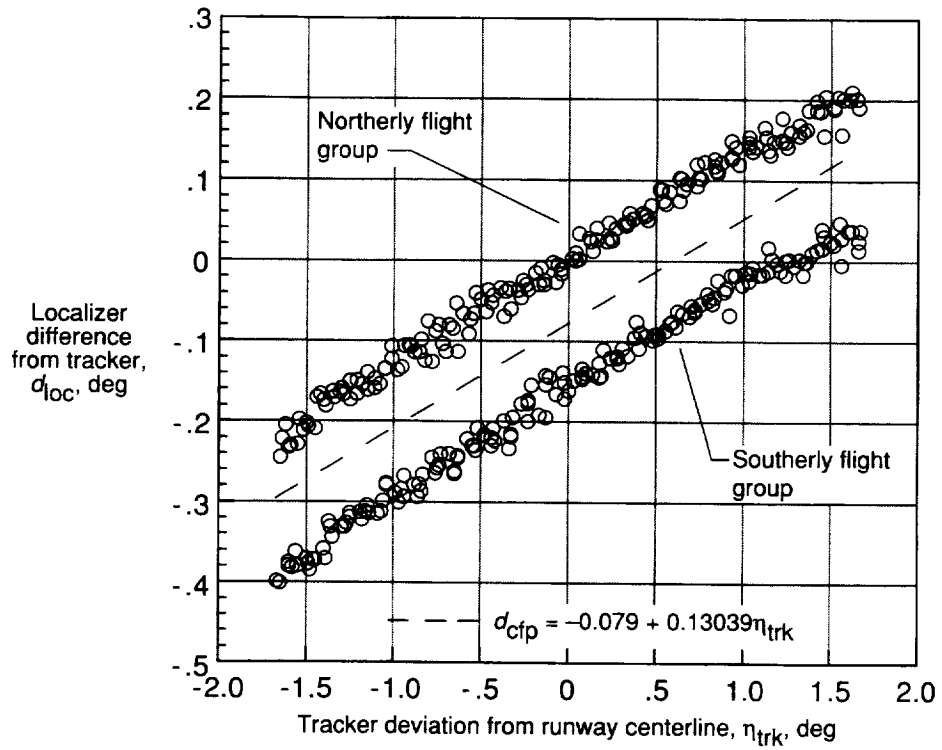


(c) Range of 14 n.mi.

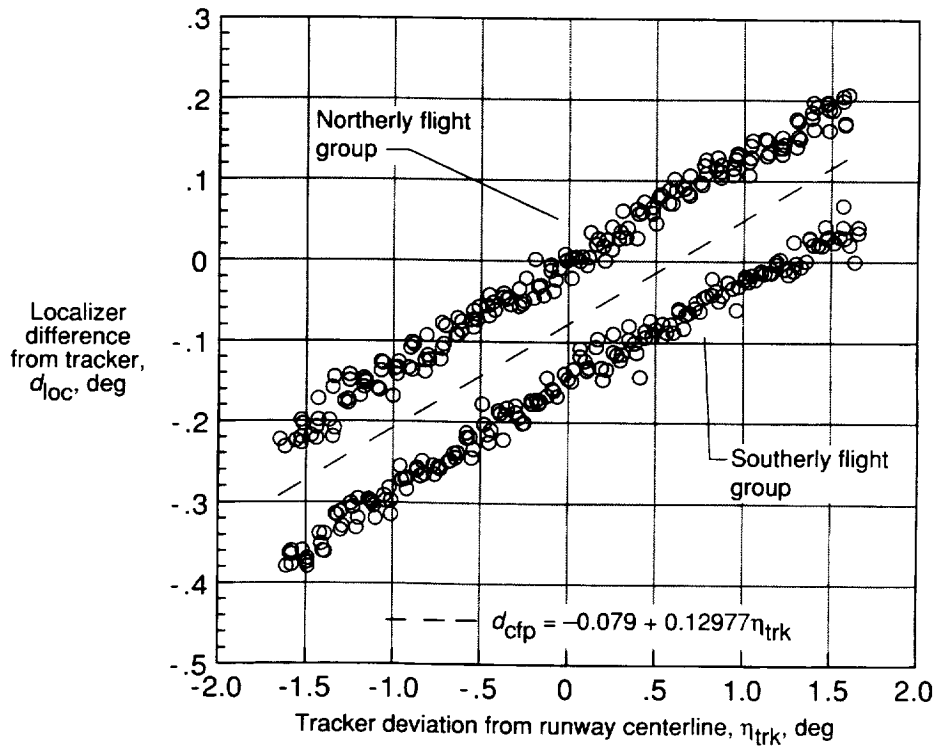


(d) Range of 16 n.mi.

Figure 10. Continued.

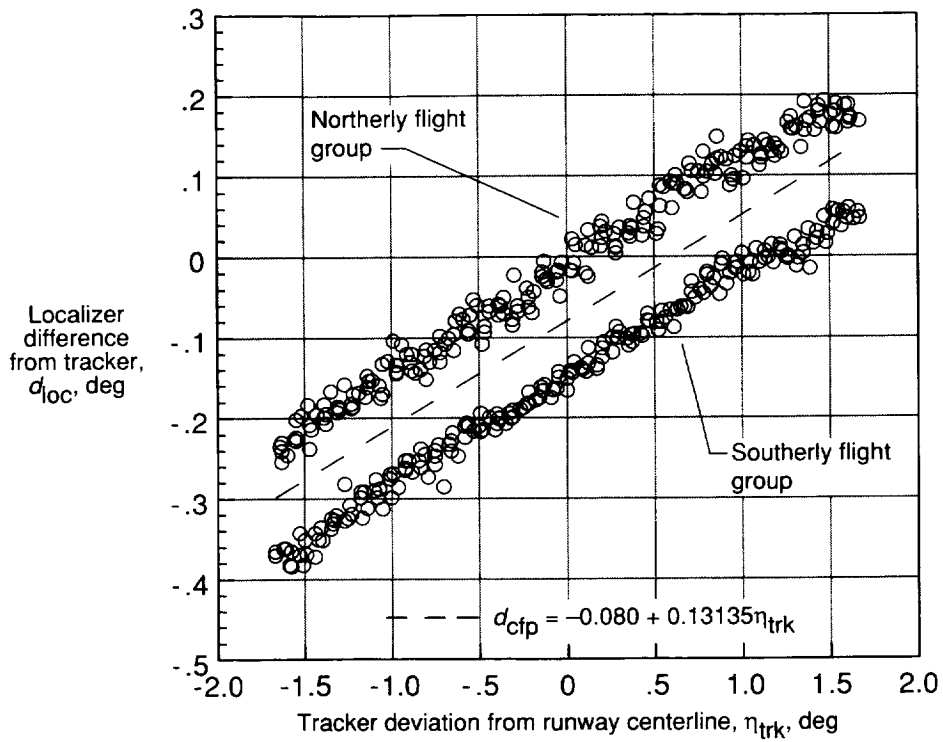


(e) Range of 18 n.mi.

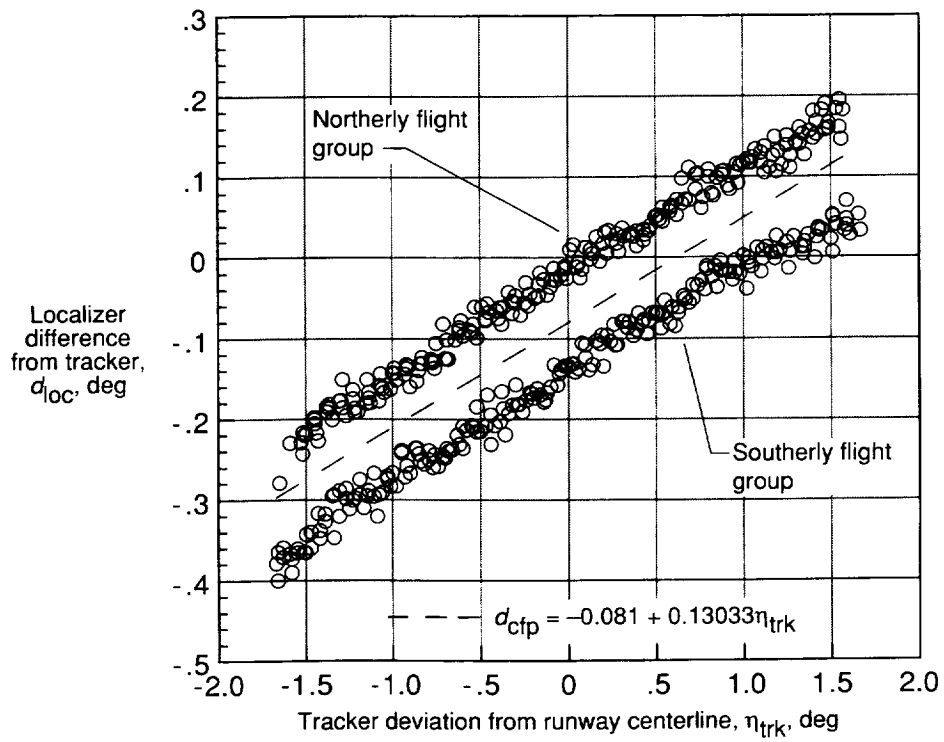


(f) Range of 20 n.mi.

Figure 10. Continued.

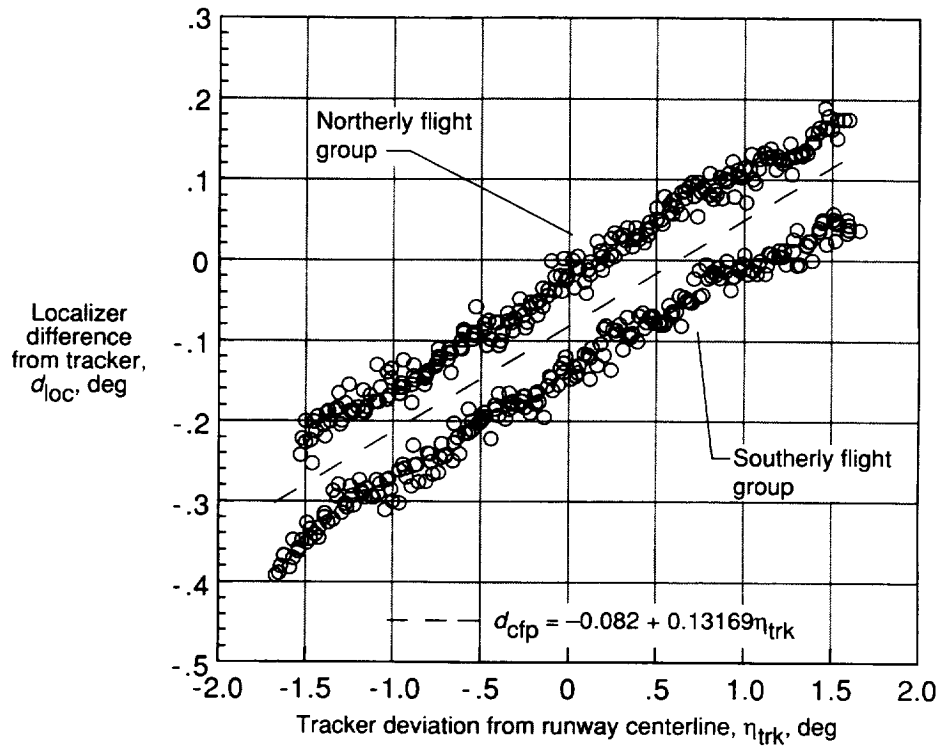


(g) Range of 22 n.mi.

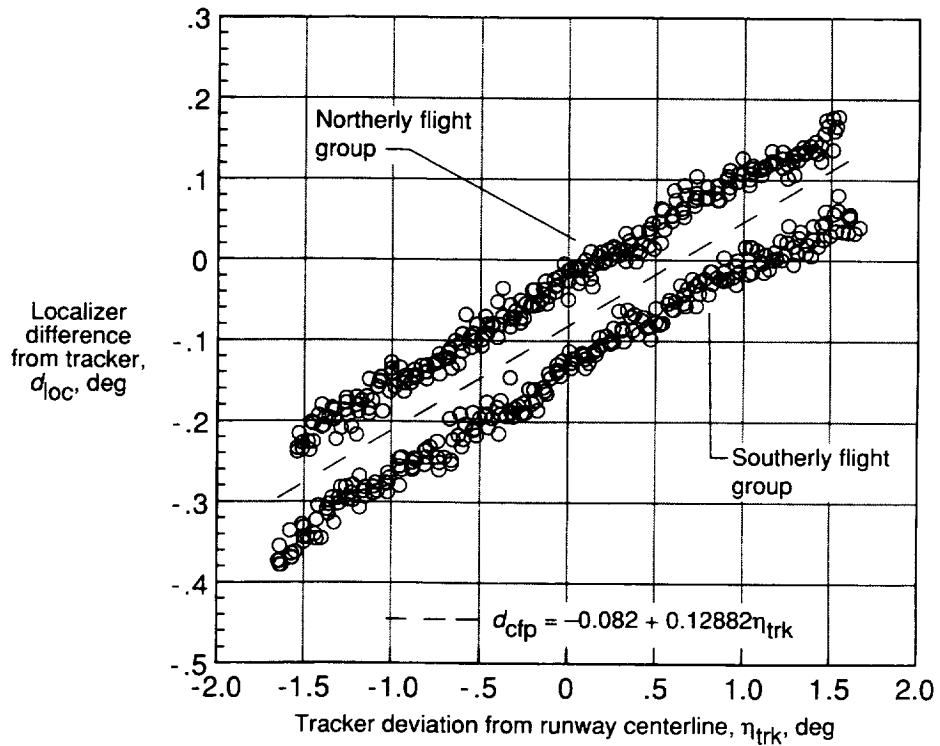


(h) Range of 24 n.mi.

Figure 10. Continued.

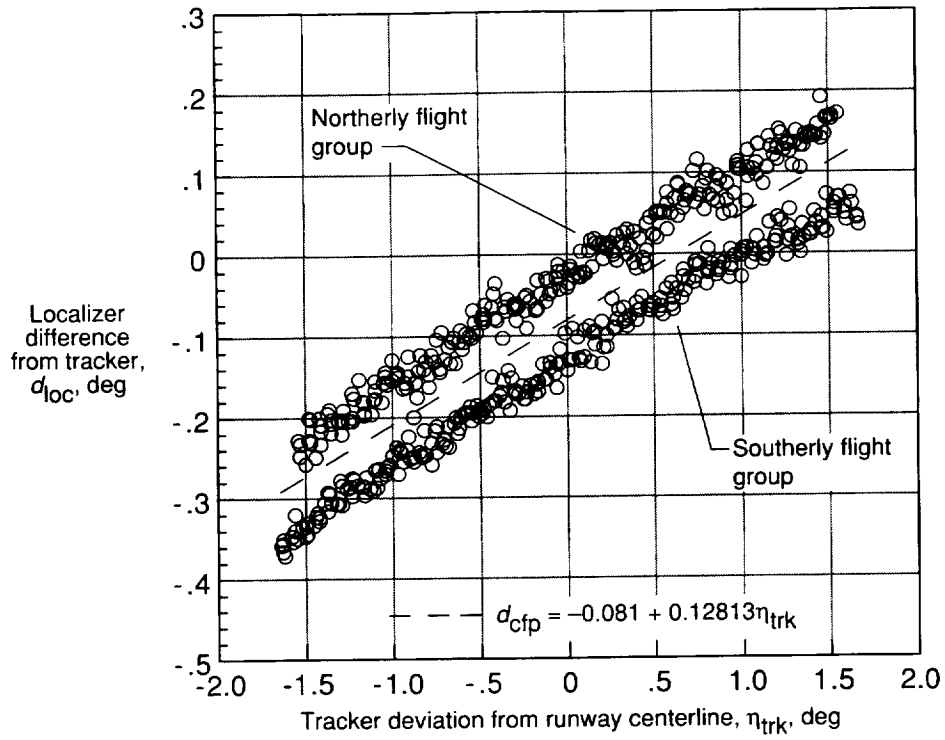


(i) Range of 26 n.mi.

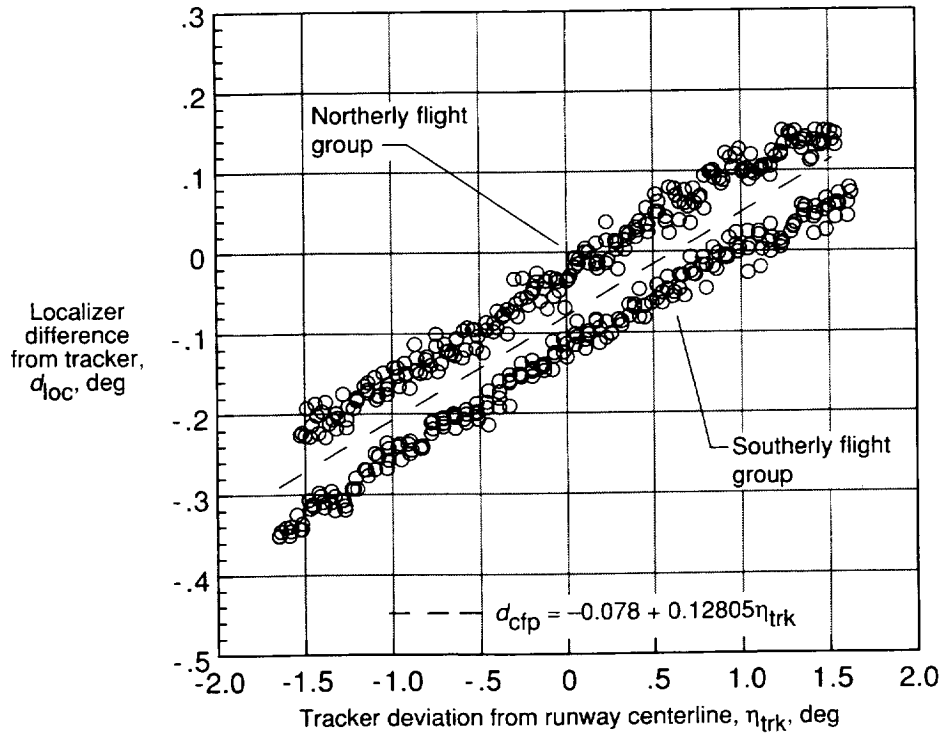


(j) Range of 28 n.mi.

Figure 10. Continued.



(k) Range of 30 n.mi.



(l) Range of 32 n.mi.

Figure 10. Concluded.

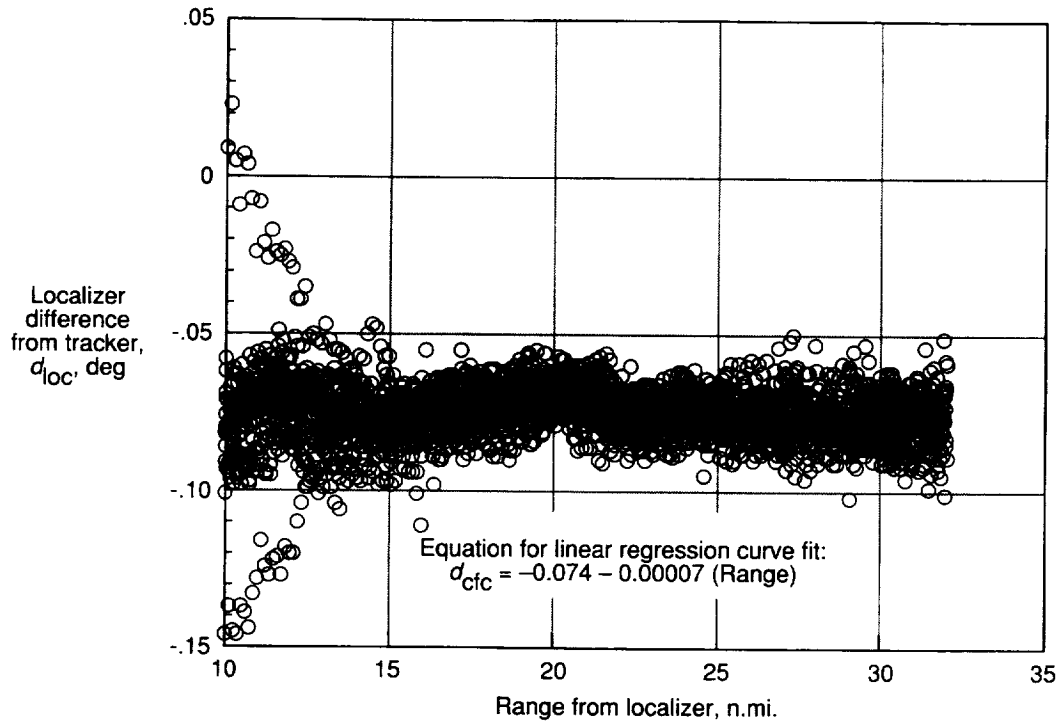


Figure 11. Localizer difference from tracker as function of range flying outbound on localizer centerline.

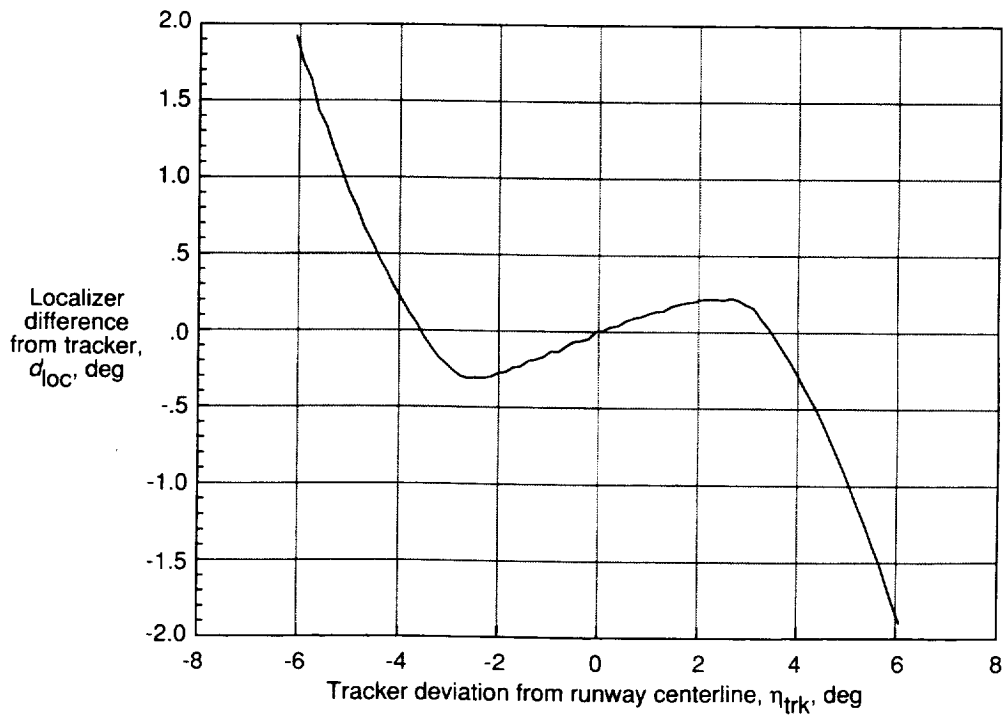


Figure 12. Localizer difference from tracker as function of tracker deviation from runway centerline at 24 n.mi.

REPORT DOCUMENTATION PAGE			Form Approved OMB No. 0704-0188	
Public reporting burden for this collection of information is estimated to average 1 hour per response, including the time for reviewing instructions, searching existing data sources, gathering and maintaining the data needed, and completing and reviewing the collection of information. Send comments regarding this burden estimate or any other aspect of this collection of information, including suggestions for reducing this burden, to Washington Headquarters Services, Directorate for Information Operations and Reports, 1215 Jefferson Davis Highway, Suite 1204, Arlington, VA 22202-4302, and to the Office of Management and Budget, Paperwork Reduction Project (0704-0188), Washington, DC 20503.				
1. AGENCY USE ONLY(Leave blank)	2. REPORT DATE November 1994	3. REPORT TYPE AND DATES COVERED Technical Memorandum		
4. TITLE AND SUBTITLE Modeling of Instrument Landing System (ILS) Localizer Signal on Runway 25L at Los Angeles International Airport			5. FUNDING NUMBERS WU 505-64-13-04	
6. AUTHOR(S) Richard M. Hueschen and Charles E. Knox				
7. PERFORMING ORGANIZATION NAME(S) AND ADDRESS(ES) NASA Langley Research Center Hampton, VA 23681-0001			8. PERFORMING ORGANIZATION REPORT NUMBER L-17334	
9. SPONSORING/MONITORING AGENCY NAME(S) AND ADDRESS(ES) National Aeronautics and Space Administration Washington, DC 20546-0001			10. SPONSORING/MONITORING AGENCY REPORT NUMBER NASA TM-4588	
11. SUPPLEMENTARY NOTES				
12a. DISTRIBUTION/AVAILABILITY STATEMENT  Unclassified-Unlimited Subject Category 04 Availability: NASA CASI (301) 621-0390			12b. DISTRIBUTION CODE	
13. ABSTRACT (Maximum 200 words) A joint NASA/FAA flight test has been made to record instrument landing system (ILS) localizer receiver signals for use in mathematically modeling the ILS localizer for future simulation studies and airplane flight tracking tasks. The flight test was conducted on a portion of the ILS localizer installed on runway 25L at the Los Angeles International Airport. The tests covered the range from 10 to 32 n.mi. from the localizer antenna. Precision radar tracking information was compared with the recorded localizer deviation data. Data analysis showed that the ILS signal centerline was offset to the left of runway centerline by 0.071° and that no significant bends existed on the localizer beam. Suggested simulation models for the ILS localizer are formed from a statistical analysis.				
14. SUBJECT TERMS Instrument landing system (ILS); Air Traffic Control (ATC); Closely spaced parallel runways; Navigation; Sensor modeling			15. NUMBER OF PAGES 29	
			16. PRICE CODE A03	
17. SECURITY CLASSIFICATION OF REPORT Unclassified	18. SECURITY CLASSIFICATION OF THIS PAGE Unclassified	19. SECURITY CLASSIFICATION OF ABSTRACT Unclassified	20. LIMITATION OF ABSTRACT	

